www.ijcps.org

IJCPS Vol. 8, Issue 3
May-Jun 2019

ISSN:2319-6602
International Journal of Chemical and Physical Sciences

SYNTHESIS OF A NOVEL TRANSITION METAL OXIDE / CONDUCTING POLYMER NANOCOMPOSITES AND STUDY OF THEIR ELECTRICAL TRANSPORT AND OPTICAL PROPERTIES

A DEY[1]

[1]Department of Chemistry, Sarsuna College, Kolkata-700061, India
Corresponding author: Ashis Dey, deyashis@gmail.com, Telefax: 0332452 3699

Abstract

In the vast field of nanotechnology, conducting polymer nanocomposites have become a prominent area of research and development for advanced materials. Matrix based nanocomposites have overlooked the field of nanotechnology but there is an ocean of great possibilities. The incorporation of inorganic nanoparticles into the polymer chain provides a unique route to design new novel materials with potential technological applications. The properties of nanocomposites are quite different from the constituent materials due to molecular level interactions. Moreover the properties can be tailored by varying the composition. Here we have made an attempt to prepare Zirconia-polyaniline (ZrO_2-PANI) nanocomposites using the colloidal stability of zirconia sol. Complex impedance and dielectric permittivity of ZrO_2-PANI nanocomposites have been investigated as a function of frequency and temperature for different compositions. Optical energy band gap of ZrO_2 decreases with the increase of polyaniline concentration. The electrical inhomogeneity induces two conduction processes, which are attributed to grain and grain boundary effects. A very large dielectric permittivity of about 2500 at room temperature has been observed for the composite with highest content of zirconia. The large dielectric permittivity arises due to interfacial polarization involving heterogeneous behavior of semiconducting zirconia and conducting polyaniline.

Keywords: Conducting polymer, nanocomposites, dielectric constant, optical band gap

INTRODUCTION

Conducting polymers (CPs) constitute an important class of organic functional materials[1, 2]. Their unique physical and electrical properties and being inexpensive, easy to synthesize, and suitable matrices for biomolecule immobilization have enabled them to find a wide range of use, including playing roles in supercapacitors[3,4], batteries[5], electrochromic devices[6], solar cells[7], sensors[8-10] and biomedical applications. To enhance the performance of the CPs, various composite materials have been synthesized with carbon-based materials, metals or metal oxides, semiconductor etc. The conducting polymers such as polyaniline (PANI), polypyrrole (PPy), polythiophene (PTh), and poly (3, 4-ethylenedioxythiophene) (PEDOT) have been explored as matrices to incorporate a number of CPs.

Zirconia (ZrO_2) is considered to be one of the most important ceramic materials due to high dielectric permittivity[11, 12] ionic conductivity and many others technological applications [13, 14, 15]. Zirconia exists in three different polymorphic form, namely cubic, tetragonal and monoclinic. The stable monoclinic phase at room temperature is transformed to the tetragonal one at 1170^0C and then to cubic[16]

at 2370^{0}C. The two high temperature phases are unstable in the bulk form at ambient temperature. Research on the metastable phases of these materials and their transition have been a subject of great scientific and technological interest in the recent decades. Tetragonal ZrO_2 are used in thermal barrier coatings because of its low thermal conductivity and thermal expansion coefficient. It is also used as ion conductors in high temperature sensors[17]. A number of explanations have been given for the stabilization of metastable tetragonal as well as cubic phase of zirconia at low temperature. The possible reasons as suggested by many research groups are due to finite crystallite size[18, 19], lattice defects[20] and oxygen anion vacancies[21] Zirconia are doped with many aliovalent cation such as Mg^{2+}, Ca^{2+} and Y^{3+} to stabilize cubic and tetragonal phase at room temperature[19]. Recently, it has been reported that zirconia nanocrystals show high ionic conductivity due to fast oxygen diffusion through grain boundary[22].

The electrical and dielectric studies of an isolated nanoparticles are very difficult to perform. In this respect, the dispersion of nanosized particles within a suitable matrix is essential to investigate the physical properties as well as to design novel materials. The combined effects of organic and inorganic compounds yield a completely different class of materials.[23] Polyaniline (PANI) is the most attractive conducting polymer due to its high electrical conductivity and thermal stability. Synthesis of zirconia nanoparticle in polyaniline[24] and polypyrrole[25, 26] and some preliminary characterizations have been reported. In this work we present the electrical and dielectric properties of PANI-ZrO_2 nanocomposites at low temperature and high frequency employing impedance spectroscopy.

EXPERIMENTAL WORK:

Ammonium peroxydisulphate (APS) and aniline were purchased from E. Merck (India). Aniline was distilled twice under reduced pressure and stored below 4^{0}C in nitrogen atmosphere to avoid aerial oxidation. APS was used as received.

ZrO_2 nanoparticles have been prepared by a standard two reverse emulsion technique.[27–29] ZrO_2 sol was prepared by dissolving a known amount (1 gm) of finely divided powder in double distilled water. The sol was dialyzed until free from all unwanted ions. The nanocomposites of polyaniline (PANI)-ZrO_2 were prepared as follows. 50 ml of ZrO_2 colloid was taken at each time and the volume was reduced to about 20 ml on evaporation at -35^{0}C using a lyophilizer. Different volume of aniline (0.1-0.5 ml) was syringed to the colloid under ultrasonic action to reduce the agglomeration of ZrO_2 nanoparticles. 1.5 M of acidic aqueous solution of ammonium peroxydisulphate, APS (precooled) using varying amount of concentrated HCl and keeping 1:1.25 monomer : APS mole ratio was then added dropwise under sonication. The polymerization was allowed to proceed for 24 hours maintaining the temperature at 0-5^{0}C. The composite came out as brilliant green residue.

Table I: Weight percentage of aniline (x), room temperature dielectric constant (ε_1) at 40 kHz

Sample	x	ε_1 (40 kHz)
C1	67.1	2500
C2	80.3	2191
C3	85.9	1563
C4	89.1	1374
C5	91.1	975
C6	100.0	362

The solution was then washed several times with 1.5 M HCl and deionized water under ultra centrifugation followed by drying in vacuum oven at 60^{0}C for 24 h to obtain fine green powder. Five

different compositions (C1-C5) with varying concentration of aniline and pure PANI (C6) as shown in Table I were characterized in details.

Characterization:

X-Ray Diffraction (XRD) pattern of the nanocomposites were performed using a Philips Diffractometer (PW 1710) using Cu K_α radiation. Particle size of the bare nanoparticles and the nanocomposites and the nature of interaction between the conducting and insulating components were determined from Scanning (SEM; Model: JEOL- JSM 6700F) and Transmission Electron Microscopic (TEM; Model: JEOL, HRTEM JEM 2010) studies. UV-Vis spectra of the stable dispersion of nanocomposites and bare nanoparticles were recorded using UV-2401PC (Shimadzu, Japan) spectrometer.

The complex dielectric function, $\varepsilon^* = \varepsilon_1 + i\varepsilon_2$ was obtained from the measurements of capacitance (C) and dissipation factor (D) by autobalance bridge 4192A Agilent Impedance Analyser up to the frequency of 1.6 MHz with an applied ac voltage of 1 V. Agilent test lead 16048A with coaxial cable at room temperature and two-electrode configuration in the cryostat for low temperatures were used. The temperature was varied from 303 K to 123 K in a liquid nitrogen cryostat using Eurotherm temperature controller, Model No. 2404. The samples for measurements were prepared by uniaxial pressure in a stainless steel die. The samples were disk shaped of 8-10 mm diameter and 0.7-1.0 mm thickness. The electrical contacts on both sides of the pelletized samples were made by silver paint. All the measurements were carried out by a computer based on general purpose interface board (GPIB). The real part of dielectric constant (ε_1) was evaluated by the relation $C = \varepsilon_0\, \varepsilon_1\, S/t$, ε_0 is the permittivity of vacuum, S is the area and t is the thickness of the sample. The imaginary component was calculated from the dissipation factor, $\varepsilon_2 = D\, \varepsilon_1$.

RESULTS AND DISCUSSIONS:

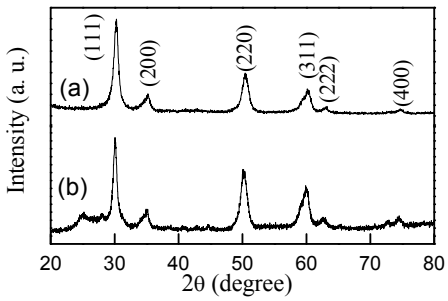

FIG. 1: X-ray diffraction pattern of (a) as synthesized ZrO_2 nanoparticles and (b) ZrO_2-PANI nanocomposite sample C1.

Fig.1 (a-b) show the characteristic peaks of X-ray diffraction (XRD) of bare ZrO_2 nanoparticles and the nanocomposite sample (C1) with highest content of ZrO_2. The main peaks at $2\theta = 30.3^o$ (111), 35.3^o (200), 50.5^o (220), 60.3^o (311), 63.0^o (222) and 74.6^o (400) which are characteristics of tetragonal

ZrO_2 are also present in the composite. A broad peak appears around 25.1° (110) which is attributed to highly doped emeraldine salt,[30] suggesting some degree of crystallinity in PANI. During polymerization the growth of polymer chain is restricted to some extent in presence of ZrO_2 nanoparticles and the polymer becomes more and more crystalline. The crystallite size of the ZrO_2 nanoparticles in the composite was calculated following the diffraction peak. At $2\theta = 30.3^o$ (111 face), which is the characteristics peak of ZrO_2, is chosen to calculate the average diameter and it comes out to be 16 nm, which is consistent with that obtained from TEM studies. Tetragonal zirconia can be stabilized at room temperature without doping when the particle Scherrer's equation[31]

$$D = K\lambda / \beta \cos\theta \quad (1)$$

where K = 0.89, D represents crystallite size (nm), λ, the wavelength of CuK_α radiation and β, the corrected value at half width (FWHM) of the size is less than 30 nm.[32, 33]. The size effect is attributed to the lower surface free energy of the tetragonal form as compared to that of the monoclinic phase. As a result of it the tetragonal phase becomes more predominant for nanosized particles. In the present investigation the ZrO_2 nanoparticles having size less than 30 nm is thermodynamically favorable for the stabilization of metastable tetragonal phase.

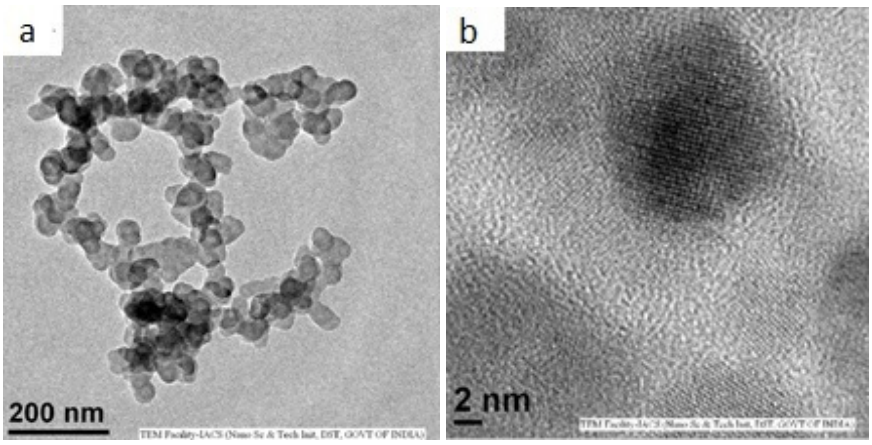

FIG 2: TEM micrograph of (a) lower magnification image of C1 and (c) high resolution lattice image of C1 in the background of PPY matrix.

Fig. 2 (a-b) shows the Transmission electron micrograph (TEM) of the nanocomposite sample with highest (C1) loading of ZrO_2. Fig. 2 (a) shows the lower magnification image of the sample C1 which indicates the nanoparticles to be well dispersed in the polymer matrix and are of spherical shape with uniform diameter. Fig 2 (b) is the high resolution transmission electron micrograph (HRTEM) of C1 (15-28 nm). This shows the lattice image from a ZrO_2 nanoparticle in the surrounding of PPY matrix. The lattice spacing is found to be 0.127 nm, which corresponds to (400) plane in ZrO_2. After the formation of the composites the particles (dark shaded) are found to be encapsulated into polypyrrole (light shaded) chains. So it can easily be concluded that the polymer are formed on the surface of the individual nanoparticles.

Fig. 3 (a) and 3 (b) exhibit the scanning electron micrograph (SEM) of the nanocomposite sample with highest (C1) and lowest (C4) loading of ZrO_2 respectively. SEM reveals that the grain size are of the

order of 40-180 nm and it go on decreasing with the increasing of ZrO_2 content in the nanocomposites. The grain morphology appears more uniform with the increase of ZrO_2 content.

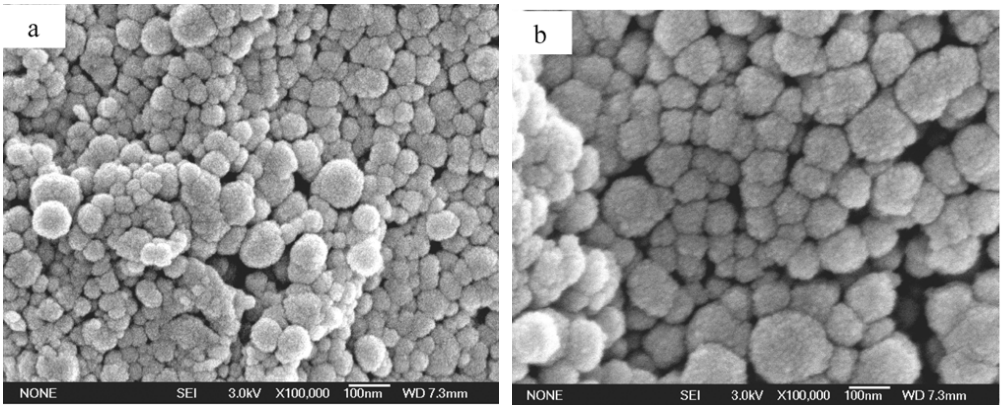

Fig. 3: SEM micrograph of the cold pressed powder samples (a) C1 and (b) C4 respectively.

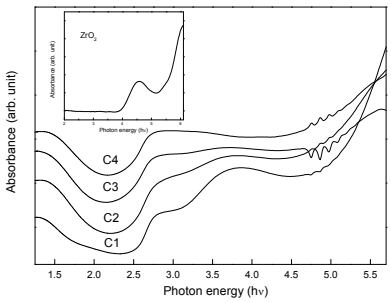

FIG. 4: Electronic absorption spectra of the four different nanocomposites (C1-C4) samples. The inset shows the same for pure ZrO_2 nanoparticles

The UV-VIS absorption spectra of the diluted colloidal composite dispersions of two samples (C1 and C3) are shown in Fig.4. The characteristics bands of conducting form of polyaniline (emeraldine salt) appear at 3.8, 1.8 and 1.3 eV, which are attributed to π-π*, polaron-π* and π-polaron transitions respectively.[34,35] An additional peak appears at 2.8 eV for all the composites samples indicating PANI in highly doped state. The absence of any peak around 2 eV associated with the quinoid rings eliminates the possibility of formation of insulating form (emeraldine base). The inset shows the same for bare ZrO_2 nanoparticles. A strong absorption starts at around 3.8 eV. The band gap corresponding to the band edge structure gives activation energy of 4.0 eV, which is lower compare to the optical band gap of bulk zirconia as reported earlier.[36] This indicates that there is contribution from extrinsic states, such as surface trap or defects states (possible due to Zr^{3+}). The absorption coeffcient α is assessed for the three samples from the equation[37] $\alpha = 2.303 \times 10^3 A\rho/lc$ where A is the sample absorbance, ρ is the density of ZrO_2, c is the sample concentration in g/liter, and l is the path length.

The optical absorption coeffcient (α) near the absorption edge of the semiconductor can be described as[38]

$$\alpha h\nu = A\,(h\nu - E_g)^{m} \qquad (2)$$

where A is the absorption constant, photon energy is hν, h is the plank constant and E_g is optical band gap. Generally the optical band gap in a semiconductor is determined by assuming the nature of the transition (m) and plotting $(\alpha h\nu)^{1/m}$ vs hν where m represents the nature of the transition. Now m may have different values, such as 1/2, 2, 3/2 or 3 for allowed direct, allowed indirect, forbidden direct and forbidden indirect transitions respectively. For allowed direct transition one can plot $(\alpha h\nu)^2$ vs. hν as presented in Fig. 3 and extrapolate the linear portion of it to α= 0 value to obtain the corresponding band gap. In this case m = 1/2 and so the interband transition is allowed direct. The estimated band gap for ZrO_2 is 5.12 eV and it decreases from 5.05 eV (C1) to 4.25 eV (C5) with increasing concentration of polyaniline.

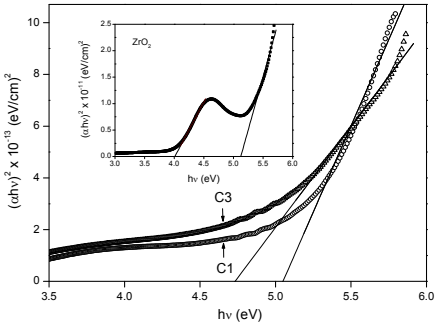

FIG. 4: Plot of $(\alpha h\nu)^2$ vs photon energy (hν) for the two nanocomposites samples (C1-C3) and the inset is for bare ZrO_2 nanoparticles.

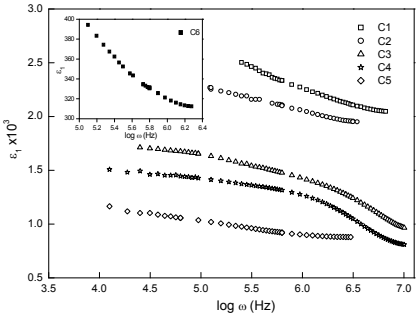

FIG. 5: Frequency dependence of the real part of relative dielectric permittivity (ε_1) at room temperature for the five samples. Inset shows the same for the sample C6.

Zirconia is a direct band gap insulator with two distinct band to band transitions at 5.2 eV and 5.79 eV.[39] The highest occupied molecular orbitals (HOMOs) of the valence band are formed by overlapping 2p states of oxygen ions with some admixing of 4d orbital of Zr^{4+} ions. The lowest unoccupied molecular orbitals (LUMOs) of the conduction band originate from 4d orbitals of Zr^{4+} ions

with some admixing of 2p orbitals of oxygen.[40]. The absorption band at 5-6 eV originates due to the transitions from 2p states of oxygen to 4d states of zirconia.

The dielectric constant, ε_1 as a function of frequency at room temperature for different compositions are presented in Fig. 5. The inset shows the same for pure PANI. The magnitude and the frequency dependence of ε_1 are strongly dependent on the content of ZrO_2 nanoparticles. In case of more conducting samples, the value of ε_1 is almost independent of frequency. The most important finding is that the nanocomposites exhibit a very high dielectric constant of about 2503 at room temperature for the sample with highest content of ZrO_2. The value of dielectric constant in ZrO_2 varies from 15 to 40 depending on the various crystalline phases.[37,38] Theoretically it is established that lattice contribution gives a high value of dielectric constant compared to electronic effect. The value of ε_1 for PANI is approximately 400. The present observation of ε_1 is remarkable as it is larger than the constituent materials by six times.

CONCLUSION

Zirconia nanoparticles of size 15–30 nm reveal a tetragonal crystalline phase at room temperature. TEM shows the particles are not simply blended with the polymer rather they are entrapped in the polymer matrix. The concentration of ZrO_2 has a remarkable effect on the dielectric properties of the nanocomposites. Optical energy band gap of ZrO_2 decreases with the increase of polyaniline concentration. The electrical inhomogeneity induces two conduction processes, which are attributed to grain and grain boundary effects. Higher dielectric constant results from the heterogeneous behavior of semiconducting zirconia and conducting polyaniline which induces Maxwell–Wagner Polarization in the nanocomposites.

REFERENCES

[1] R. Gangopadhyay and A. De, *Chem. Mater,* 12, 608 (2000).
[2] H. S. Nalwa (editor) Handbook of Organic-Inorganic Hybrid Materials and Nanocomposites, Chapter H conducting Polymer Nanocomposites, R. Gangopadhyay and A. De. (American Scientific Publishers, 2003).
[3] M. Li, Y. Zhang, L. Yang, Y. Liu, J. Ma, *J. Mater. Sci.: Mater. Electron*. 26, 485–492 (2015).
[4] K. Lota, G. Lota, A. Sierczynska, I. Acznik, *Synth. Met*. 203, 44–48 (2015).
[5] Y. Gao, H.-L. Yip, K.-S. Chen, K. M. O'Malley, O. Acton, Y. Sun, G. Ting, H. Chen, A. K. -Y. Jen, *Adv. Mater*. 23, 1903–1908 (2011).
[6] F. Alvi, M. K. Ram, P. A. Basnayaka, E. Stefanakos, Y. Goswami, A. Kumar, *Electrochim. Acta* 56, 9406–9412 (2011).
[7] M. Sekkarapatti Ramasamy, A. Nikolakapoulou, D. Raptis, V. Dracopoulos, G. Paterakis, P. Lianos, *Electrochim. Acta* 173, 276–281 (2015).
[8] L. Huang, Y. Huang, J. Liang, X. Wan, Y. Chen, *Nano Res.* 4, 675–684 (2011).
[9] H. Randriamahazaka, J. Ghilane, *Electroanalysis,* 28, 13–26 (2016).
[10] N. Yang, G. M. Swain, X. Jiang, *Electroanalysis* 28, 27–34 (2016).

[11] G. D. Wilk, R. M. Wallace, J. M. Anthony, *J. Appl. Phys.* 89, 5243 (2001).
[12] V. V. Afanasev, M. Houssa, A. Stesmans, M. M. Heyns, *Appl. Phys. Lett*. 78, 3073 (2001).
[13] S. P. S. Badwal, *Appl. Phys. A* 50, 449 (1990).
[14] T. M. Miller, V. H. Grassian, *J. Am. Chem. Soc.* 117, 10969 (1995).
[15] J. F. Haw, J. Zhang, K. Shimizu, T. N. Venkatraman, D. P. Luigi, W. Song, D. H. Barich, J. B. Nicholas, *J. Am. Chem. Soc.* 122, 12561 (2000).
[16] T. Uchikoshi, Y. Sakka, K. Ozawa and K. Hiraga, *J. Mater. Res.* 13, 840 (1998).
[17] K. Schindler, D. Schmeisser, U. Vohrer, H. D. Wiemhofer and W. Gopel, *Sens. Actuators*. 17, 555 (1989).
[18] R. C. Garvie, *J. Phys. Chem*. 69, 1238 (1965).
[19] R. C. Garvie, *J. Phys. Chem.* 82, 218 (1978).
[20] F. Wu and S. Wu, *J. Mater. Sci. 25*, 970 (1990).
[21] S. P. S. Badwal, M. J. Bannister and R. H. J. Hannink (editor) Science and Technology of Zirconia V, P. Kountouros and G. Petzow (Technomic Publishing Company, Lancaster, PA, 1993, p30).
[22] H. L. Tuller, *Solid State Ionics*. 131, 143 (2000).
[23] X. Guo, E. Vasco, S. Mi, K. Szot, E. Wachsman and R. Waser, *Acta. Mater*. 53, 5161 (2005).
[24] S. S. Ray and M. Biswas, *Synth. Met*., 108, 231 (2000).
[25] A. De, A. Das and S. Lahiri, *Synth. Met*., 144, 303 (2004).
[26] A. Bhattachayya, K.M. Ganguly, A. De, S. Sarkar, *Mater. Res. Bull.*, 31, 527 (1996).
[27] Y. X. Pang and X. Bao, *J. Mater. Chem*., 12, 3699 (2002).
[28] L. Gao, H. C. Qiao, H. B. Qiu and D. S. Yan, *J. Eur. Ceram. Soc*., 16, 437 (1996).
[29] K. Osseo-Asare, Microemulsion-mediated Synthesis of Nanosize Oxide Materials, Handbook of Microemulsion Science and Technology, P. Kumar and K. L. Mittal (editor), Marcel Dekker Inc., New York, 1999.
[30] J. P. Pouget, M. E. Jozefowicz, A. J. Epstein, X. Tang and A. G. Macdiarmid, *Macromolecules* 24, 779 (1991).
[31] H. P. Klug and L. E. Alexander, X-ray diffraction procedures for polycrystalline and amorphous materials, John Wiley and Sons, New York, 1954, p491.
[32] R. C. Garvie, *J. Phys. Chem*. 69, 1238 (1965).
[33] R. C. Garvie and M. F. Goss, *J. Mater. Sci.*, 21, 1253 (1986).
[34] A. Raghunathan, T. S. Natarajan, G. Rangarajan, S. K. Dhawan and D. C. Trivedi, *Phy. Rev. B*., 47, 13189 (1993).
[35] S. Stafstrom, J. L. Bredas, A. J. Epstein, H. S. Woo, D. B. Tanner, W. S. Huang and A. G. MacDiarmid, *Phy. Rev. Lett*., 59, 1464 (1987).
[36] A. Emeline, G. V. Kataeva, A. S. Litke, A. V. Rudakova, V. K. Ryabchuk and N. Serpone, *Langmuir* 14, 5011(1998).
[37] N. Serpone, D. Lawless and R. Khairutdinov, *J. Phys . Chem* 99, 16646 (1995).
[38] J. I. Pankove, Optical Processes in Semiconductors, Prentice Hall, New Jersey, 1971.
[39] C. K. Kwok and C. R. Aita, *J. Appl. Phys*., 66, 2756 (1989).
[40] C. Morant, A. Fernandez and A. R. Gonzalez-Elipe, L. Soriano, A. Stampfl, A. M. Bradshaw and J. M. Sanz, *Phy. Rev. B*., 52, 11711 (1995).